Hydrodeoxygenation of Methyl Laurate over Ni Catalysts Supported on Hierarchical HZSM-5 Zeolite

Nana Li [1], Yadong Bi [1,*], Xiaoqiang Xia [1], Hui Chen [1,*] and Jianli Hu [2]

[1] Tianjin Key Laboratory of Organic Solar Cells and Photochemical Conversion,
    School of Chemistry and Chemical Engineering, Tianjin University of Technology, Tianjin 300384, China;
    153135302@stud.tjut.edu.cn (N.L.); xq840520738@gmail.com (X.X.)
[2] Department of Chemical and Biomedical Engineering, West Virginia University, Morgantown, WV 26506,
    USA; john.hu@mail.wvu.edu
[*] Correspondence: byd@tjut.edu.cn (Y.B.); tjge@tjut.edu.cn (H.C.); Tel./Fax: +86-22-6021-4259 (Y.B. & H.C.)

Abstract: The hierarchical HZSM-5 zeolite was prepared successfully by a simple NaOH treatment method. The concentration of NaOH solution was carefully tuned to optimal the zeolite acidity and pore structure. Under NaOH treatment conditions, a large number of mesopores, which interconnected with the retained micropores, were created to facilitate mass transfer performance. There are very good correlations between the decline of the relative zeolite crystallinity and the loss of micropores volume. The Ni nanoclusters were uniformly confined in the mesopores of hierarchical HZSM-5 by the excessive impregnation method. The direct deoxygenation in N_2 and hydrodeoxygenation in H_2 of the methyl laurate were compared respectively over the Ni/HZSM-5 catalysts. In the N_2 atmosphere, the deoxygenation rate of the methyl laurate on the Ni/HZSM-5 catalyst is relatively slow. In the presence of H_2, the synergistic effect between the hydrogenation function of the metal and the acid function of the zeolite supports can make the deoxygenation level more obvious. The yield of hydrocarbon products gradually reached the maximum with the appropriate treatment concentration of 1M NaOH, which could be attributed to the improved mass transfer in the hierarchical HZSM-5 supports.

Keywords: hierarchical HZSM-5; Ni; hydrodeoxygenation; methyl laurate

1. Introduction

Non-edible lipids are green renewable biomass energy, mainly including algae oil [1], jatropha oil [2] and cooking waste oil. Transforming the lipid raw material into high quality fuel through catalytic technology is a hot research and development field [3–6]. The first generation technology of lipid catalysis transformation is the production of fatty acid methyl ester biodiesel via transesterification methods over homogeneous base catalyst, which is currently a mature industrial production technology. However, the restricted utilization of biodiesel is inevitable due to the shortcomings such as high oxygen content and poor anticoagulant performance. Therefore, it is necessary to develop the second generation hydrocarbon fuel technology by further deoxygenation [7]. The different pathways for the deoxygenation of fatty acids include decarboxylation, decarbonylation, and hydrodeoxygenation. The reaction rate of deoxygenation of fatty acids through direct decarboxylation or decarbonylation is slow and needs to be carried out at higher reaction temperatures. Hydrodeoxygenation of lipid in hydrogen atmosphere is a promising solution.

The catalyst for hydrodeoxygenation of lipids mainly includes Co [8], Mo [9], W [10], Fe [11], or precious metals [12–15]. Conventional supported catalysts mainly use inert silica, alumina, and carbon as supports. In recent years, Ni-based bifunctional catalysts supported on silica–alumina

zeolites have achieved satisfactory performance in the hydrodeoxygenation of lipids [16–20], by the integration of the hydrogenation function of the metal and the acid function of the supports.

Crystallized zeolites have ordered micropores, which is comparable to the reactant molecules in pore size, resulting in the large specific surface area and shape-selective catalysis. Compared with other porous materials, they exhibit high hydrothermal stability. Zeolites have been widely used in the petrochemical industry due to their tunable structure and acidity.

The diffusion and mass transfer resistance of molecules in and out of micropores often limit the space utilization in microporous zeolites. In the treatment of regenerated raw materials such as heavy oil, vegetable oils, and lignocellulosic feeds, it is necessary to optimize the accessibility of zeolites to these components. Some mesoporous zeolites have larger pore sizes, but industrial applications are hindered due to synthesis cost and poor stability. The pore structure of the hierarchical zeolite, which contains interconnected mesopores and micropores, is suitable for solving this accessibility problem. Zeolite micropores have the function of acid catalysis, while the extra creation of larger mesopores ensures the entry and mass transfer of large reactant molecules. In addition, when the zeolite is used as a support for an active component, it is possible to improve the load capacity and ensure the access of active components in the internal surface of the porous channel.

Desilication of a microporous zeolite using an alkaline solution, such as NaOH [20] or ammonia [21], creating intracrystalline mesopores through hydrolysis of the skeleton atom, is the most feasible preparation method for the hierarchical zeolite at large-scale industrial grade, which has been successfully applied to the Hβ [20], HUSY [21], and HZSM-5 [22] zeolites. Here, HZSM-5 was treated by a simple NaOH solution method. By carefully controlling the alkaline concentration, hierarchical HZSM-5 with optimal acidity and pore structure were successfully prepared. The hydrodeoxygenation of lipids over a Ni catalyst supported on the hierarchical HZSM-5 was investigated by evaluating the impact of mass transfer performance on the yield of paraffin products of methyl laurate. In so doing, new high-efficiency bifunctional catalysts of lipid hydrodeoxygenation can be further developed.

2. Results

2.1. Nitrogen Physisorption Characterization

Figure 1 shows the nitrogen adsorption/desorption isotherms of NaOH-treated HZSM-5 zeolites. Table 1 lists the corresponding specific surface area, pore volume, and average pore size. The parent HZSM-5 is characterized by typical microporous material properties, with a microporous surface area of 387 m^2/g and a negligible mesoporous surface area of 19 m^2/g. A high adsorption capacity was achieved on initial low relative pressure (p/p_0 is less than 0.01), and the isotherm then remained flat with the increase in relative pressure, indicating that the parent HZSM-5 is a microporous material with a uniform pore structure. The pore structure of HZSM-5-0.1 changed little after treatment with 0.1 M NaOH solution, while the isotherm was almost overlapped with the parent HZSM-5. The adsorption capacity of HZSM-5-0.5 increased slightly in the higher relative pressure region of the isotherm ($0.4 < p/p_0 < 0.85$). The mesoporous surface area increased to 35 m^2/g, and the corresponding microporous surface area was reduced to 371 m^2/g. The pore structure of HZSM-5-1 underwent great changes. The adsorption capacity increases continuously with the relative pressure, indicating the creation of pores with a wider pore size. At the same time, a significant hysteresis loop appears in the region with relative pressure of $0.4 < p/p_0 < 0.85$ on the isotherm, which indicates the presence of the intracrystalline mesopores characterized by the typical type IV isotherm of mesoporous materials. At this time, the mesoporous surface area increased significantly to 126 m^2/g, while the microporous surface area decreased to 300 m^2/g. When the concentration of NaOH increased to 1.5 M, the adsorption capacity on the isotherm at the initial relatively low relative pressure decreased significantly (p/p_0 is less than 0.01), but there was a rapid increase in the high-pressure region (p/p_0 is greater than 0.85). The mesoporous surface area and microspore surface area of HZSM-5-1.5 decreased

to 63 m^2/g and 161 m^2/g, respectively. The microporous structure was destroyed, while some of the intergranular macropores were produced.
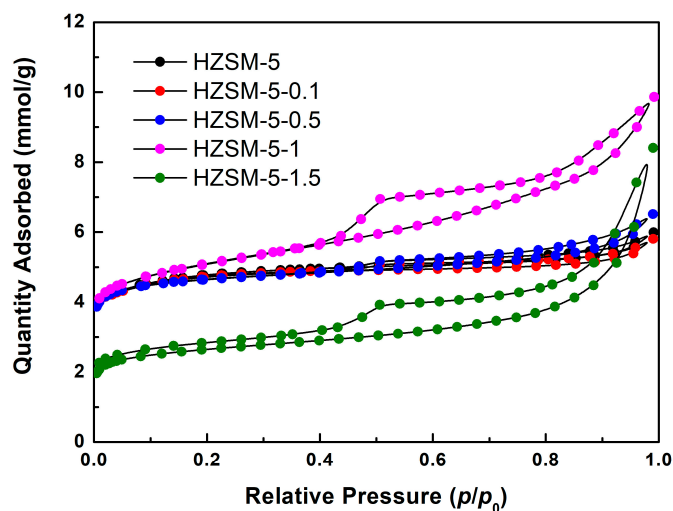

Figure 1. N$_2$ physisorption (at 77 K) isotherms for parent HZSM-5 and the hierarchical HZSM-5 treated with different concentrations of NaOH solution (0.1–1.5 M) at 343 K for 1 h.

Table 1. Physicochemical properties of parent HZSM-5 and the hierarchical HZSM-5 treated with different concentrations of NaOH solution (0.1–1.5 M) at 343 K for 1 h.

Sample	NaOH Concentration (mol/L)	S$_{Meso}$ (m^2/g)	S$_{Micro}$ (m^2/g)	V$_{Meso}$ (cm^3/g)	V$_{Micro}$ (cm^3/g)	Rel. Crystal. (%)
HZSM-5	0	19	387	0.05	0.16	100
HZSM-5-0.1	0.1	13	388	0.04	0.16	83
HZSM-5-0.5	0.5	35	371	0.08	0.15	78
HZSM-5-1	1	126	300	0.21	0.12	54
HZSM-5-1.5	1.5	63	161	0.22	0.06	45

Figure 2 shows the pore size distribution calculated from the adsorption branch of the isotherms using the BJH method. The additional NaOH treatment clearly resulted in a pore width of 5–15 nm for the formed mesopores in the hierarchical HZSM-5 zeolites. Especially for HZSM-5-1, the derived pore size distributions reveal that the newly formed pores were very uniform small mesopores, centered around 5 nm. Furthermore, the pore diameters shifted to large mesopores, around 15–30 nm when the NaOH concentration was1.5 M.
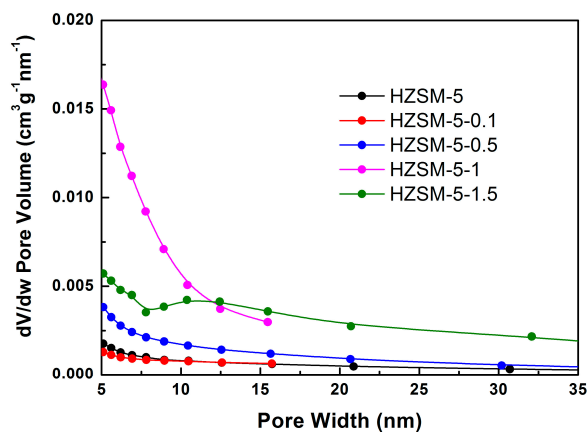

Figure 2. Pore size distribution of parent HZSM-5 and the hierarchical HZSM-5 treated with different concentrations of NaOH solution (0.1–1.5 M) at 343 K for 1 h.

Under NaOH treatment conditions, the lager mesopores were created by the amorphization and framework atom leaching to the filtrate [21]. Due to the strong alkaline nature of the NaOH solution, the treatment condition was very harsh with high pH values of 12.7–13.3 (0.05–0.2 M). The concentration of NaOH had to be controlled in a certain range due to the compromise between the formation of mesopores and the retention of micropores. A large number of mesopores, which interconnected with micropores, were created to facilitate mass transfer performance. However, excessive concentration of NaOH sometimes caused the micropores of HZSM-5 to disappear in large numbers.

2.2. Structural XRD Characterization

Figure 3 shows the XRD patterns of NaOH-treated HZSM-5. The typical diffraction peaks of the parent HZSM-5 located at 22.4 degrees. With the increase of NaOH concentration, the crystal structure of the hierarchical HZSM-5 was basically maintained. At the same time, the intensity of the diffraction peak decreased gradually, indicating the decrease of the relative crystallinity of HZSM-5 [21]. The relative crystallinity was calculated according to the intensity of the typical diffraction peak located at 22.4 degrees, assuming that the crystallinity of the parent HZSM-5 material was 100%. For example, when the NaOH concentration was 1 M, the relative crystallinity was only 54% of the parent HZSM-5. There is a very good correlation between the decline of the relative crystallinity and the loss of microporous volume.
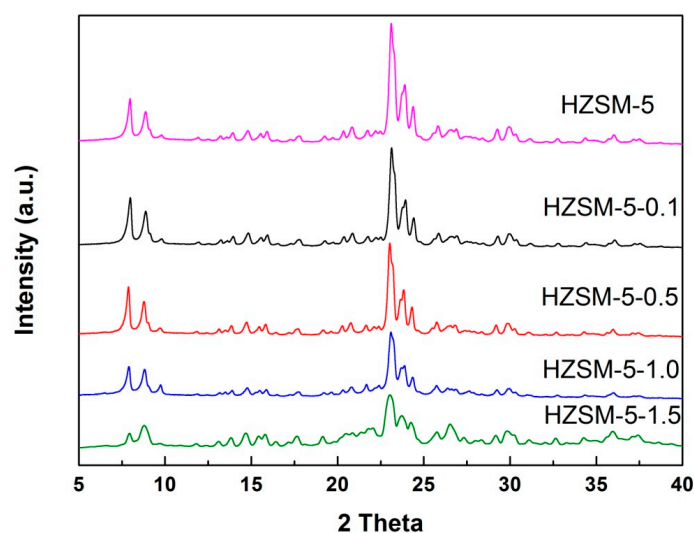

Figure 3. XRD patterns for parent HZSM-5 and the hierarchical HZSM-5 treated with different concentrations of NaOH solution (0.1–1.5 M) at 343 K for 1 h.

Figure 4 shows the XRD patterns of Ni/HZSM-5 catalysts after the reduction. For Ni catalyst supported on NaOH-treated HZSM-5, only the characteristic peaks of Ni^0 metal were observed on the XRD diffraction patterns, indicating that the pretreatment conditions can reduce the impregnated nickel species completely. Zhao Chen [20] had previously reported that Ni nanoparticles were mainly deposited on the outer surface for the microporous HBEA zeolite. While high loading Ni nanoclusters can be uniformly confined in the mesopores for the hierarchical HBEA zeolite.
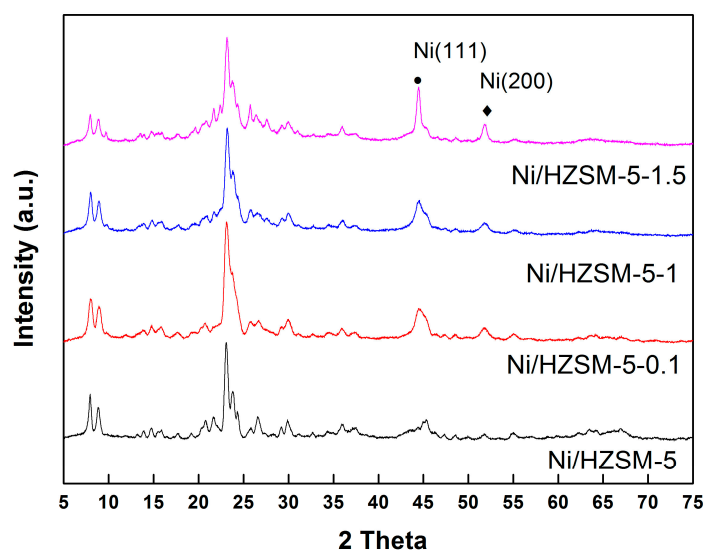
Figure 4. XRD patterns for reduced Ni catalysts supported over parent HZSM-5 and the hierarchical HZSM-5.

2.3. NH$_3$-TPD Characterization

Figure 5 shows the NH$_3$-TPD patterns of HZSM-5 treated with NaOH. Two ammonia desorption peaks can be observed, in which the low temperature peak is due to the weakly adsorbed ammonia molecules via hydrogen bonding, instead of the acid sites [21]. The high temperature peaks can be attributed to strong Bronsted acid sites. It had been previously reported that the alkaline treatment of HZSM-5 may not significantly decrease the acidity. FT-IR measurement of adsorbed pyridine verified that a large part of Lewis acid sites, which formed in the partial desilication, was selectively removed by the following acid treatment [23]. During our NaOH treatment process, Na$^+$ ions were exchanged into the cationic sites of the HZSM-5 samples. The Bronsted acidity could be recovered by following ion exchanging with NH$_4^+$. Thus, Bronsted acid sites mainly exist over NaOH-treated hierarchical HZSM-5.
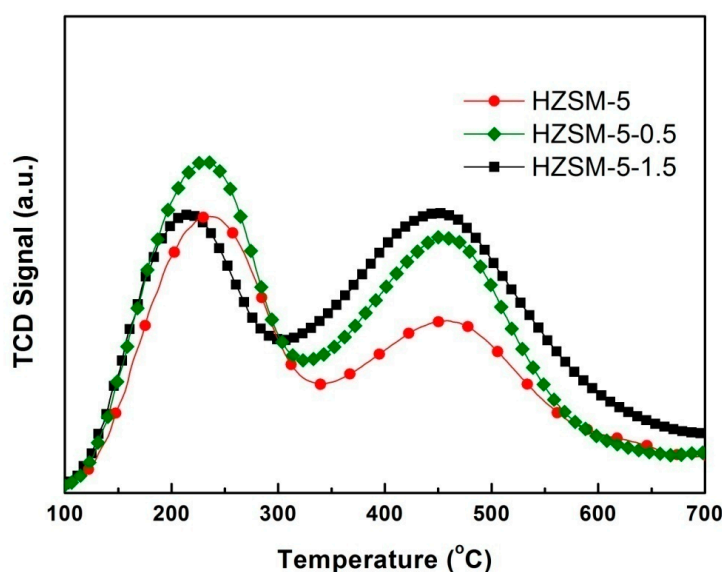

Figure 5. NH$_3$-TPD profiles for parent HZSM-5 and the hierarchical HZSM-5 treated with different concentrations of NaOH solution (0.5 and 1.5 M) at 343 K for 1 h.

With the increase in NaOH concentration, the low temperature peak did not change. Although the desorption temperature of the high temperature peak remained essentially unchanged, the peak area gradually increased. This indicates that NaOH treatment has little effect on the strength of the Bronsted acid sites, but the Si/Al ratio increases with the desilication under alkaline conditions. The Bronsted acid sites are mainly due to the Al in the framework, so the number of Bronsted acid sites per unit mass of catalyst increases.

2.4. Transmission Electron Microscopic Observation

Figure 6 shows the typical TEM micrographs for 10 wt % Ni catalysts supported over the parent HZSM-5 and the hierarchical HZSM-5-1. The mean sizes of Ni particles in both samples were similar and were distributed in a range of 8–11 nm by counting ca. 50–100 particles. Similar particle sizes for impregnated metal (Ru or Ni) supported over various hierarchical zeolites have been proposed in previous studies [20,21], suggesting that the hierarchical zeolite itself plays crucial roles in reaction activity. Table 2 summarizes the physicochemical properties of the Ni/HZSM-5 catalysts.
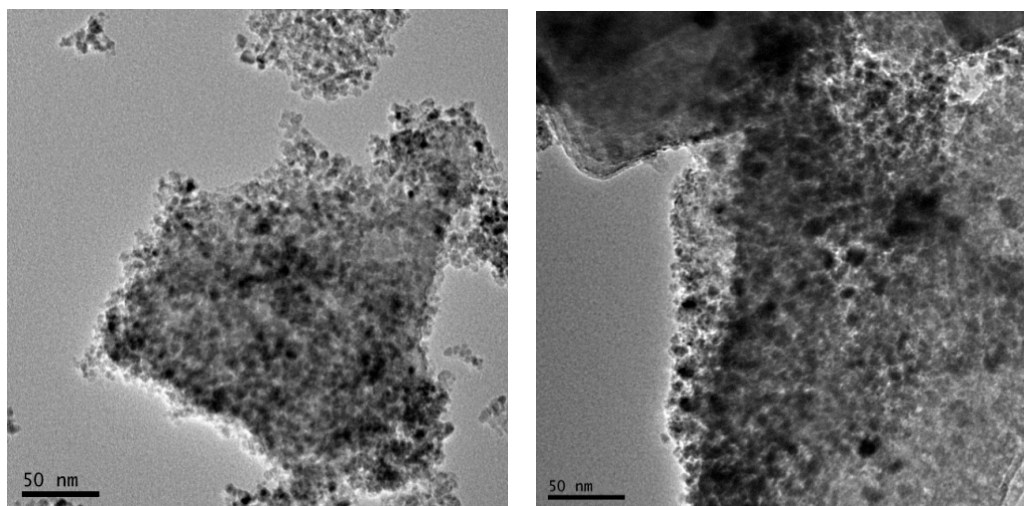

Figure 6. Transmission electron micrograph of Ni/HZSM-5 (**left**) and Ni/HZSM-5-1 (**right**) catalysts.

Table 2. Physicochemical properties of Ni catalysts supported over parent HZSM-5 and the hierarchical HZSM-5 treated with different concentrations of NaOH solution (0.1–1.5 M) at 343 K for 1 h.

Catalyst	Si/Al (mol/mol) [a]	d_{Ni} (nm) [b]	S_{BET} (m²/g)
Ni/HZSM-5	22	8–11	259
Ni/HZSM-5-0.1	-	-	284
Ni/HZSM-5-1	14.2	8–11	232
Ni/HZSM-1.5	-	-	286

[a] Determined by EDX analysis. [b] Determined by TEM micrographs.

2.5. Deoxygenation of Methyl Laurate over Ni HZSM-5 Catalysts in N_2

Table 3 summarizes the comparison of methyl laurate conversion over 10 wt % Ni catalysts loaded on the hierarchical HZSM-5. Figure 7 shows the product distribution of methyl laurate conversion in the N_2 atmosphere. In the nitrogen atmosphere, the conversion of methyl laurate over the parent Ni/HZSM-5 catalyst was 25.4%, and the main products were lauric acid and a small amount of undecane. With the increase in NaOH concentration, the conversion of methyl laurate over treated Ni/HZSM-5 catalysts gradually increased. The highest conversion was 61.5% for Ni/HZSM-5-1, and the corresponding yield of lauric acid and undecane were 26.3% and 5.9%. However, when the

treatment concentration of NaOH increased to 1.5 M, the conversion of methyl laurate and the yield of lauric acid decreased to 50.5% and 19.6%, respectively.

Table 3. Comparison of methyl laurate conversion over 10 wt % Ni catalysts loaded on the hierarchical HZSM-5 treated with different concentrations of NaOH solution (0.1–1.5 M).

Catalyst	Atmosphere	Conversion (%)	Yield (wt %)			
			Oxygenates	C12	C11	Cracking
Ni/HZSM-5	N_2	25.4	11.8	-	2.5	-
Ni/HZSM-5-0.1	N_2	39.6	16.9	-	4.3	-
Ni/HZSM-5-0.5	N_2	54.2	21.0	-	5.2	-
Ni/HZSM-5-1	N_2	61.5	26.3	-	5.9	-
Ni/HZSM-1.5	N_2	50.5	19.6	-	6.8	-
Ni/HZSM-5	H_2	86.2	6.4	26.3	18.6	4.4
Ni/HZSM-5-0.1	H_2	87.6	3.6	26.3	19.3	4.7
Ni/HZSM-5-0.5	H_2	87.8	6.2	28.6	21.0	4.2
Ni/HZSM-5-1	H_2	89.8	2.6	37.6	27.7	10
Ni/HZSM-1.5	H_2	68.7	4.6	13.2	9.1	4.6

Experimental conditions: methyl laurate (3.5 mmol), n-hexane (20 mL), catalyst (0.1 g), 280 °C, 2 MPa of N_2 or H_2 (room temperature), and stirring at 600 rpm for 5 h.
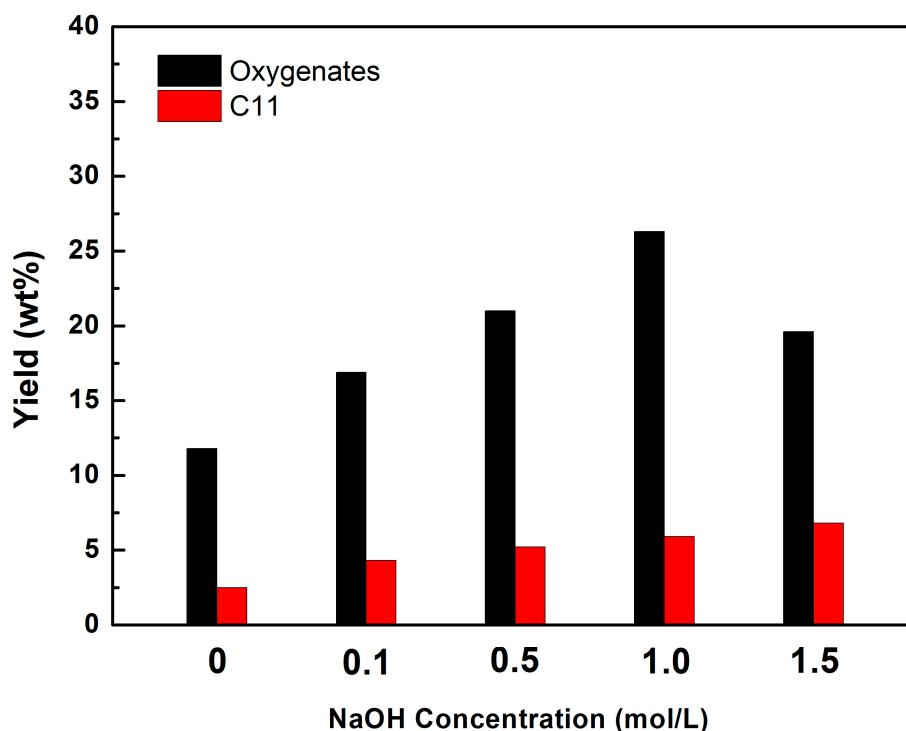

Figure 7. Yields for deoxygenation of methyl laurate in N_2 over 10 wt % Ni catalysts loaded on the hierarchical HZSM-5 treated with different concentrations of NaOH solution (0.1–1.5 M). Experimental conditions: methyl laurate (3.5 mmol), n-hexane (20 mL), catalyst (0.1 g), 280 °C, 2 MPa of N_2 (Room temperature), and stirring at 600 rpm for 5 h.

In a nitrogen atmosphere, methyl laurate can hydrolyze to lauric acid, while the undecane is derived from the direct decarboxylation of lauric acid [24]. The decarboxylation rate of fatty acids on the Ni/HZSM-5 catalyst was relatively slow, so the yield of undecane was very low. The acidity of the zeolite supports had little contribution to the direct decarboxylation reaction. The increase in methyl laurate conversion can be attributed to the improved mass transfer in the hierarchical HZSM-5 supports, which well correlate with the trend of the surface area of the mesopores.

2.6. Hydrodeoxygenation of Methyl Laurate over Ni/HZSM-5 Catalysts in H_2

Figure 8 shows the products distribution of methyl laurate conversion in the H_2 atmosphere. According to Table 3, in the hydrogen atmosphere, the conversion of methyl laurate was significantly higher than that of nitrogen. The conversion of methyl laurate on the Ni/HZSM-5 catalyst was 86.2%. The product distribution was more complicated than that in the nitrogen atmosphere. In terms of hydrocarbon products, in addition to undecane, dodecane, some isoparaffin, and some cracking alkane products were distributed. In terms of oxygenate products, in addition to a small amount of lauric acid, dodecanal and dodecanol, which were not produced in the nitrogen atmosphere, were distributed. With the increase in NaOH treatment concentration, the conversion of methyl laurate on the Ni/HZSM-5 catalyst almost remained unchanged until the NaOH concentration was 1 M. The yield of undecane and dodecane products gradually increased, which reached a maximum of 65.3% when the NaOH concentration was 1 M. However, when the NaOH concentration increased to 1.5 M, the conversion of methyl laurate decreased to 68.7%, while the yield of undecane and dodecane was reduced to 22.3%. Compared with the nitrogen atmosphere, the yield of the oxygenate products was remarkably reduced in the hydrogen atmosphere, whereas a small amount of cracking hydrocarbons was produced.

In a hydrogen atmosphere, the hydrogenolysis of methyl laurate generates lauric acid. The deoxidation of lauric acid proceeds via more complex reaction paths: (1) First, tandem hydrogenation to intermediate oxygenates, such as dodecanal and dodecanol, and then to dodecane through dehydration/hydrogenation of dodecanol, which is an alkane with the same number carbon atoms as the fatty acid; (2) Direct decarboxylation/decarbonylation of the oxygenates (acid, aldehyde or alcohol) to undecane, which is one carbon atom less than the fatty acids [25]. The deoxygenated alkanes can be transformed into isoparaffins and light hydrocarbons by isomerization and cracking reaction. For the Ni/HZSM-5 bifunctional catalyst, the main function of metal Ni is to catalyze the hydrogenolysis of methyl laurate, the decarbonylation of aldehyde/alcohol, and the hydrogenation of acids/aldehyde, while that of Bronsted acid sites from the HZSM-5 supports is to catalyze the dehydration of fatty alcohols and the isomerization and cracking of alkanes.

The yield of dodecane was significantly higher than that of undecane in alkane products. In a hydrogen atmosphere, over Ni catalysts supported on acidity Zeolite, the predominant reaction path is the tandem hydrogenation of lauric acid carboxyl group to form dodecanal/dodecanol intermediates, and further the dehydration/hydrogenation of alcohol to dodecane, instead of the metal-catalyzed decarbonylation of the dodecanal to undecane.

With the increase of the concentration of NaOH, the molar ratio of dodecane to undecane, which is the ratio of hydrodeoxygenation to direct deoxidation, was maintained at approximately 1.4, indicating relative equilibrium between the amount of Bronsted acid sites and the metal active sites for the hierarchical Ni/HZSM-5 catalysts. Zhao had reported that the main product of hydrodeoxygenation of stearic acid on a Ni/HBEA bifunctional catalyst was octadecane, with low heptadecane selectivity, indicating that the main reaction route was stearic acid hydrogenation to the corresponding fatty alcohol, followed by tandem dehydration–hydrogenation, which is consistent with our results [20]. The increase in hydrocarbon (C11 and C12) yield with NaOH concentration can be ascribed to the improved mass transfer in the mesopores space of the hierarchical HZSM-5 supports. When the NaOH concentration increased to 1.5 M, due to the destruction of the microporous structure and the formation of the amorphous phase, a large number of active sites disappeared, resulting in a substantial decrease in methyl laurate conversion. In the presence of hydrogen, the direct decarboxylation/decarbonylation rate of fatty acid, aldehyde, or alcohol was promoted.
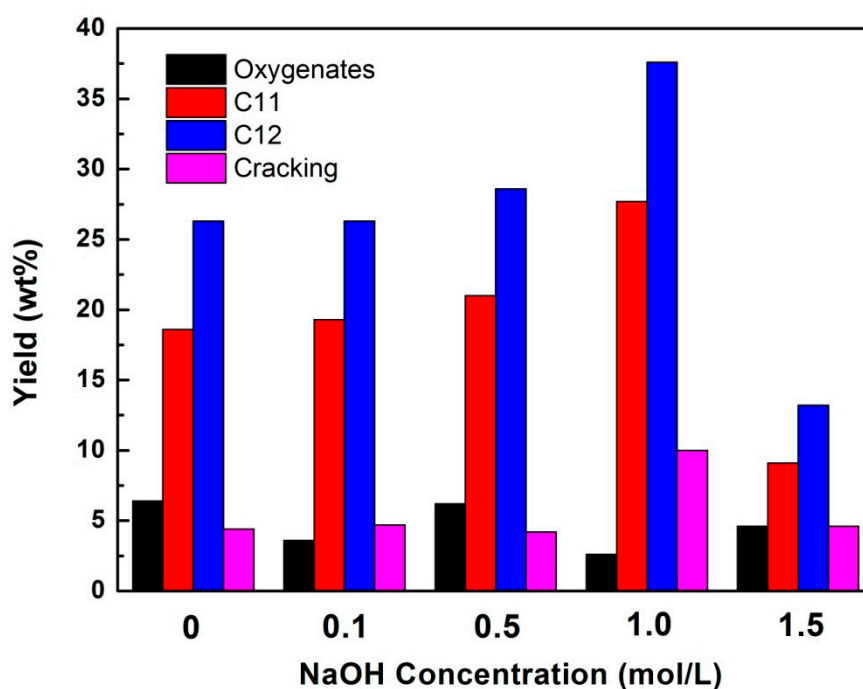
Figure 8. Yields for hydrodeoxygenation of methyl laurate in H_2 over 10 wt % Ni catalysts loaded on the hierarchical HZSM-5 treated with different concentrations of NaOH solution (0.1–1.5 M). Experimental conditions: methyl laurate (3.5 mmol), n-hexane (20 mL), catalyst (0.1 g), 280 °C, 2 MPa of H_2 (Room temperature), and stirring at 600 rpm for 5 h.

In addition, the dehydration–hydrogenation initiated by Bronsted acid function made the level of deoxygenation more obvious. Due to the high deoxygenation rate of the oxygenates, only trace amounts of aldehyde or alcohol could be detected. Dodecanal and dodecanol were present in the reaction system as key intermediate species of carboxylic acid hydrogenation. The literature reports that the dodecanal and dodecanol can be easily transformed in the equilibrium state [26]. At the same time, the cracking hydrocarbons products also increased. A large number of Bronsted acid sites catalyze the hydroisomerization and hydrocracking reaction.

3. Discussion

Figure 9 shows the influence of reaction atmosphere on methyl laurate conversion over 10 wt % Ni catalysts loaded on the hierarchical HZSM-5. First, methyl laurate was converted to lauric acid via hydrolysis or hydrogenolysis. The hydrolysis reaction catalyzed by the acidic zeolite dominated in the N_2 atmosphere. The strength of the Bronsted acid sites of NaOH-treated HZSM-5 zeolites almost remained unchanged. The enhancement of mass transfer ability of mesopores promoted the hydrolysis reaction rate. Therefore, the formation of oxygenate (mainly lauric acid) increased with the mesopore amount. Even whenHZSM-5-1.5 had a substantially damaged microporous structure, the methyl laurate conversion was still higher than that of the parent HZSM-5 due to the higher mesoporous volume. The subsequent lactic acid decarboxylation occurred under the catalysis role of metallic nickel, so the generation of undecane was inconsistent with the variation trend of the mesopore. In the H_2 atmosphere, hydrogenolysis reaction catalyzed by metal Ni particles dominated in the H_2 atmosphere. Since the reaction rate of hydrogenolysis was much faster than the hydrolysis step, the methyl laurate conversion in the H_2 atmosphere had an advantage over the N_2 atmosphere. The methyl laurate conversion was almost unchanged for the hierarchical HZSM-5 treated with different concentrations of NaOH solution (0.1–1 M), except for the HZSM-5-1.5 with a substantially damaged microporous structure. The conversion of the methyl laurate was substantially decreased by the increased size of

the loaded metallic nickel particles. In the H_2 atmosphere, given the pivotal role of acidic zeolites, the dehydration reaction of lauric acid was also affected by the mass transfer performance. Therefore, the formation of dodecane was also consistent with the variation trend of the mesopores, reaching a maximum when the treatment concentration of NaOH was 1.0 M.
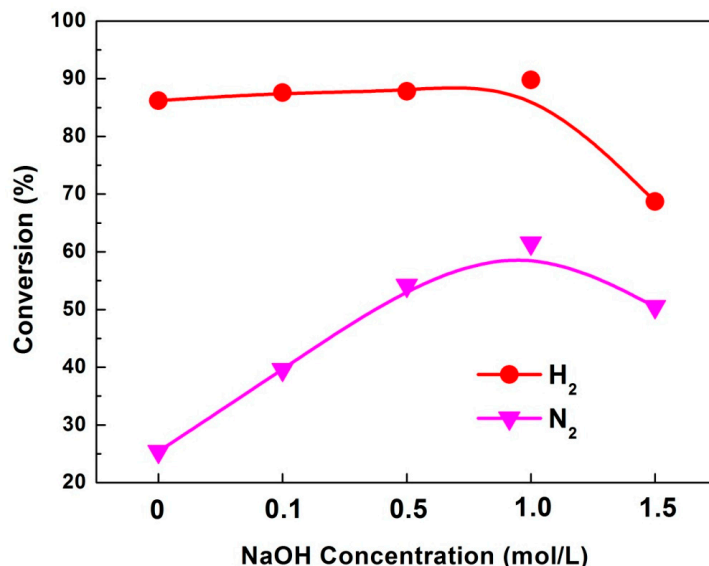

Figure 9. Influence of reaction atmosphere on methyl laurate conversion over 10 wt % Ni catalysts loaded on the hierarchical HZSM-5 treated with different concentrations of NaOH solution (0.1–1.5 M). Experimental conditions: methyl laurate (3.5 mmol), n-hexane (20 mL), catalyst (0.1 g), 280 °C, 2 MPa of N_2 or H_2 (room temperature), and stirring at 600 rpm for 5 h.

In the N_2 atmosphere, the total yield of products was significantly lower than the conversion of methyl laurate, indicating that the carbon balance was much worse than that in the H_2 atmosphere. Coke or light carbon-containing components (such as methanol, methane, and CO_x) may be produced in the reaction process, which calls for further analysis and measurement.

4. Materials and Methods

4.1. Materials and Chemicals

The HZSM-5 zeolite with a Si/Al ratio of 25 was obtained from Nankai University Catalyst Co. Ltd. (NKC, Tianjin, China). The chemical reagents $Ni(NO_3)_2 \cdot 6H_2O$ (99%, Sinopharm, Shanghai, China), hexane (98%, Aladdin, Shanghai, China), methyl laurate (99%, Aladdin, Shanghai, China), n-tetradecane (99%, Aladdin, Shanghai, China), lauric acid (98%, Aladdin, Shanghai, China), lauryl alcohol (98%, Aladdin, Shanghai, China), undecane (98%, Aladdin, Shanghai, China), and dodecane (99.5%, Aladdin, Shanghai, China) were used without further purification.

4.2. Catalyst Preparation

The hierarchical HZSM-5 was prepared by treating the HZSM-5 using NaOH aqueous solutions [21]. Typically, HZSM-5 powders (5.0 g) were added into NaOH aqueous solutions (40 mL) with different concentrations (0.1–1.5 M). Then, the suspension was heated to 343 K and stirred at 343 K for 1 h. After cooled down to room temperature, the solid was recovered by filtration and washed thoroughly with deionized water. The recovered solid sample was further exchanged to H-form with an aqueous solution of NH_4NO_3, followed by drying at 373 K for 8 h and calcination in air at 573 K for 3 h. The hierarchical HZSM-5 was denoted as HZSM-5-x, where x was the corresponding concentration among the NaOH aqueous solutions.

The 10% Ni-based catalysts were prepared by the excessive impregnation method [8]. In a typical synthesis, $Ni(NO_3)_2 \cdot 6H_2O$ (2.9 g, 0.01 mol) and citric acid (3.84 g, 0.02 mol) were dissolved in distilled water (20 mL), and the carriers (5.86 g) were then added into the mixed solution with stirring. After impregnation, the mixture was kept at 20 °C for 12 h and dried at 90 °C for 12 h. At last, the catalysts were calcined in the flowing N_2 at 500 °C for 5 h and reduced in flowing H_2 at 500 °C for 4 h.

4.3. Catalyst Characterization

BET surface area, pore size, and pore volume were measured by the physisorption method using nitrogen as absorbent at 77 K (TriStar 3020, Micromeritics, Norcross, GA, USA). The specific surface area S_{BET} was determined from the linear portion of the BET plot ($0.01 < p/p_0 < 0.08$). The total pore volume was calculated by means of the total amount of adsorbed gas at $p/p_0 = 0.98$. The mesopore portion was evaluated by the *t*-plot method. Prior to the physisorption measurements, the samples were degassed in vacuum at 573 K for 3 h to remove physically adsorbed components.

X-ray powder diffraction (XRD) patterns of the prepared samples were measured on a Philips CM-1 (Cu Kα, $\lambda = 0.1543$ nm) powder X-ray diffractometer (Panalytical, Almelo, The Netherlands). Typically, the data was collected from 10° to 80° (2θ) for conventional wide-angle XRD patterns. The software X'Pert Highscore was used to perform microstructure analysis.

Temperature-programmed desorption of NH_3 (NH_3-TPD) were carried out in an automatic chemisorb analyzer (ChemiSorb 2720, Micromeritics, Norcross, GA, USA). One hundred milligrams of each sample was introduced into a U-shaped tubular quartz reactor. Each sample was first treated at 573 K for 1 h and then cooled down to room temperature in He. NH_3 was absorbed at 393 K for 30 min (5 mL/min) of 10% NH_3/He followed by a He purge. TPD experiments were performed under a flow of He (25 mL/min) from 393 to 973 K at a constant heating rate (10 K/min). The desorbed NH_3 was monitored with a thermal conductivity detector (TCD).

Transmission electron microscopic (TEM) images of the powder samples were obtained in a JEM-2100F microscope (JOEL, Tokyo, Japan) operating at 200 KV. Si/Al ratios of the samples were determined using EDX analysis.

4.4. Catalyst Testing

Experiments were performed in a 100 mL batch reactor (Parr, Moline, IL, USA). The reactor was charged with 3.5 mmol methyl laurate feed, 100 mg of catalyst, and 20 mL of n-hexane solvent. Before reaction, the reactor was purged by N_2 to remove air residue and was then pressurized to 2 MPa of N_2 or H_2. The system was then heated to 280 °C and kept at this temperature for 5 h.

The liquid product was analyzed by a gas chromatograph-mass spectrometer and quantified by a gas chromatograph equipped with an FID detector and an HP-5MS column, using n-tetradecane as the internal standard.

The conversion is given as the weight of converted reactant per weight of the starting reactant multiplied by 100%. The yield in (wt %) is given as the weight of each product per weight of the starting reactant multiplied by 100%.

$$\text{Conversion } (\%) = \left(1 - \frac{m_{\text{Reactant,t}}}{m_{\text{Reactant,0}}} \right) \times 100.$$

$$\text{Yield } (\text{wt } \%) = \frac{m_{\text{Product,t}}}{m_{\text{Reactant,0}}} \times 100.$$

5. Conclusions

Desilication of microporous zeolite by alkaline solution post-processing is the most feasible preparation method for the hierarchical zeolite at large-scale industrial grade. Here, by carefully controlling the NaOH solution concentration, hierarchical HZSM-5 with an optimal acidity and

pore structure was prepared successfully. The crystallinity of the microporous HZSM-5 zeolite was maintained while a large number of interconnected mesopores were created. However, excessive concentration of NaOH caused the micropores of HZSM-5 to disappear in large numbers. In the nitrogen atmosphere, the increase in methyl laurate conversion can be attributed to the improved mass transfer in the hierarchical HZSM-5 supports. In a hydrogen atmosphere, the yield of the oxygenate products was, remarkably, further reduced via hydrodeoxygenation. Under optimal NaOH treatment conditions, the maximal hydrocarbon products yield of 65.3% can be ascribed to the equilibrium between the Bronsted acidity and mass transfer in the mesopore space of the hierarchical HZSM-5 supports.

Author Contributions: H.C. and J.H. conceived and designed the experiments; N.L. and X.X. performed the experiments; N.L. and Y.B. analyzed the data; Y.B. and J.H. wrote the paper.

Conflicts of Interest: The authors declare no conflict of interest.

References

1. Zhao, C.; Bruck, T.; Lercher, J.A. Catalytic deoxygenation of microalgae oil to green hydrocarbons. *Green Chem.* **2013**, *15*, 1720–1739. [CrossRef]

2. Guo, J.H.; Xu, G.Y.; Shen, F.; Fu, Y.; Zhang, Y.; Guo, Q.X. Catalytic conversion of Jatropha oil to alkanes under mild conditions with a Ru/La(OH)$_3$ catalyst. *Green Chem.* **2015**, *17*, 2888–2895. [CrossRef]

3. Gosselink, R.W.; Hollak, S.A.; Chang, S.W.; Van, H.J.; de Jong, K.P.; Bitter, J.H.; van Es, D.S. Reaction pathways for the deoxygenation of vegetable oils and related model compounds. *ChemSusChem* **2013**, *6*, 1576–1594. [CrossRef] [PubMed]

4. Dupont, J.; Suarez, P.A.Z.; Meneghetti, M.R.; Meneghetti, S.M.P. Catalytic production of biodiesel and diesel-like hydrocarbons from triglycerides. *Energy Environ. Sci.* **2009**, *2*, 1258–1265. [CrossRef]

5. Smith, B.; Greenwell, H.C.; Whiting, A. Catalytic upgrading of tri-glycerides and fatty acids to transport biofuels. *Energy Environ. Sci.* **2009**, *2*, 262–271. [CrossRef]

6. Lestari, S.; Mäkiarvela, P.; Beltramini, J.; Lu, G.Q.; Murzin, D.Y. Transforming triglycerides and fatty acids into biofuels. *ChemSusChem* **2009**, *2*, 1109–1119. [CrossRef] [PubMed]

7. Gosselink, R.W.; Stellwagen, D.R.; Bitter, J.H. Tungsten-Based Catalysts for Selective Deoxygenation. *Angew. Chem. Int. Ed.* **2013**, *52*, 5089–5092. [CrossRef] [PubMed]

8. Liu, Q.Y.; Bie, Y.W.; Qiu, S.B.; Zhang, Q.; Sainio, J.; Wang, T.J.; Ma, L.L.; Lehtonen, J. Hydrogenolysis of methyl heptanoate over Co based catalysts: Mediation of support property on activity and product distribution. *Appl. Catal. B-Environ.* **2014**, *147*, 236–245. [CrossRef]

9. Han, J.X.; Duan, J.Z.; Chen, P.; Lou, H.; Zheng, X.M. Molybdenum Carbide-Catalyzed Conversion of Renewable Oils into Diesel-like Hydrocarbons. *Adv. Synth. Catal.* **2011**, *353*, 2577–2583. [CrossRef]

10. Hollak, S.A.W.; Gosselink, R.W.; van Es, D.S.; Bitter, J.H. Comparison of Tungsten and Molybdenum Carbide Catalysts for the Hydrodeoxygenation of Oleic Acid. *ACS Catal.* **2013**, *3*, 2837–2844. [CrossRef]

11. Kandel, K.; Anderegg, J.W.; Nelson, N.C.; Chaudhary, U.; Slowing, I.I. Supported iron nanoparticles for the hydrodeoxygenation of microalgal oil to green diesel. *J. Catal.* **2014**, *314*, 142–148. [CrossRef]

12. Yang, L.Q.; Tate, K.L.; Jasinski, J.B.; Carreon, M.A. Decarboxylation of Oleic Acid to Heptadecane over Pt Supported on Zeolite 5A Beads. *ACS Catal.* **2015**, *5*, 6497–6502. [CrossRef]

13. Rozmyslowicz, B.; Maki-Arvela, P.; Tokarev, A.; Leino, A.R.; Eranen, K.; Murzin, D.Y. Influence of Hydrogen in Catalytic Deoxygenation of Fatty Acids and Their Derivatives over Pd/C. *Ind. Eng. Chem. Res.* **2012**, *51*, 8922–8927. [CrossRef]

14. Verma, D.; Kumar, R.; Rana, B.S.; Sinha, A.K. Aviation fuel production from lipids by a single-step route using hierarchical mesoporous zeolites. *Energy Environ. Sci.* **2011**, *4*, 1667–1671. [CrossRef]

15. Wang, C.X.; Tian, Z.J.; Wang, L.; Xu, R.S.; Liu, Q.H.; Qu, W.; Ma, H.J.; Wang, B.C. One-Step Hydrotreatment of Vegetable Oil to Produce High Quality Diesel-Range Alkanes. *ChemSusChem* **2012**, *5*, 1974–1983. [CrossRef] [PubMed]

16. Chen, N.; Gong, S.F.; Qian, E.W. Effect of reduction temperature of NiMoO$_{3-x}$/SAPO-11 on its catalytic activity in hydrodeoxygenation of methyl laurate. *Appl. Catal. B-Environ.* **2015**, *174*, 253–263. [CrossRef]

17. Ma, B.; Hu, J.B.; Wang, Y.M.; Zhao, C. Ni nanoparticles encapsulated into mesoporous single-crystalline HBEA: Application for drainage oil hydrodeoxygenation to diesel. *Green Chem.* **2015**, *17*, 4610–4617. [CrossRef]

18. Ma, B.; Yi, X.F.; Chen, L.; Zheng, A.M.; Zhao, C. Interconnected hierarchical HUSY zeolite-loaded Ni nano-particles probed for hydrodeoxygenation of fatty acids, fatty esters, and palm oil. *J. Mater. Chem.* **2016**, *4*, 11330–11341. [CrossRef]

19. Peng, B.X.; Yuan, X.G.; Zhao, C.; Lercher, J.A. Stabilizing Catalytic Pathways via Redundancy: Selective Reduction of Microalgae Oil to Alkanes. *J. Am. Chem. Soc.* **2012**, *134*, 9400–9405. [CrossRef] [PubMed]

20. Ma, B.; Zhao, C. High-grade diesel production by hydrodeoxygenation of palm oil over a hierarchically structured Ni/HBEA catalyst. *Green Chem.* **2015**, *17*, 1692–1701. [CrossRef]

21. Van Aelst, J.; Verboekend, D.; Philippaerts, A.; Nuttens, N.; Kurttepeli, M.; Gobechiya, E.; Haouas, M.; Sree, S.P.; Denayer, J.F.M.; Martens, J.A. Catalyst Design by NH$_4$OH Treatment of USY Zeolite. *Adv. Funct. Mater.* **2015**, *25*, 7130–7144. [CrossRef]

22. Kang, J.C.; Cheng, K.; Zhang, L.; Zhang, Q.H.; Ding, J.S.; Hua, W.Q.; Lou, Y.C.; Zhai, Q.G.; Wang, Y. Mesoporous Zeolite-Supported Ruthenium Nanoparticles as Highly Selective Fischer-Tropsch Catalysts for the Production of C5–C11 Isoparaffins. *Angew. Chem. Int. Ed.* **2011**, *50*, 5200–5203. [CrossRef] [PubMed]

23. Hiroshi, M.; Toshiyuki, Y.; Hiroyuki, I.; Seitaro, N.; Junko, N.K.; Takashi, T. Effect of desilication of H-ZSM-5 by alkali treatment on catalytic performance in hexane cracking. *Appl. Catal. A Gen.* **2012**, *449*, 188–197. [CrossRef]

24. Peng, B.X.; Zhao, C.; Kasakov, S.; Foraita, S.; Lercher, J.A. Manipulating Catalytic Pathways: Deoxygenation of Palmitic Acid on Multifunctional Catalysts. *Chem. Eur. J.* **2013**, *19*, 4732–4741. [CrossRef] [PubMed]

25. Chen, J.X.; Shi, H.; Li, L.; Li, K.L. Deoxygenation of methyl laurate as a model compound to hydrocarbons on transition metal phosphide catalysts. *Appl. Catal. B-Environ.* **2014**, *144*, 870–884. [CrossRef]

26. Peng, B.X.; Yao, Y.; Zhao, C.; Lercher, J.A. Towards Quantitative Conversion of Microalgae Oil to Diesel-Range Alkanes with Bifunctional Catalysts. *Angew. Chem. Int. Ed.* **2012**, *51*, 2072–2075. [CrossRef] [PubMed]